

An investigation into vibration analysis for detecting faults in vehicle steering outer tie-rod

Yousif Alaraji¹, Sina Alp²

¹ Yousif Alaraji; Istanbul Okan University, Faculty of Engineering, Department of Automotive Mechatronic Engineering, Istanbul, Turkey

² Sina Alp, Istanbul Okan University, Faculty of Engineering, Department of Electrical & Electronics Engineering, Istanbul, Turkey

ABSTRACT

This study presents a novel fault detection method in car gear steering systems, employing MSC Adams and MATLAB simulations to analyze angular acceleration from the outer tie rod. The approach closely mimics real accelerometer data to differentiate between normal and faulty conditions, including wear and obstacle navigation. Emphasis is on noise robustness, utilizing advanced noise injection and denoising techniques. The efficacy of wavelet scattering, discrete wavelet transform (DWT) methods, and classifiers like Support Vector Machines (SVM) and Neural Networks (NN) is extensively evaluated. Among fifteen fault detection methods, the combination of wavelet scattering with Long Short-Term Memory (LSTM) Neural Networks, optimized with Adam tuning, is notably stable across four scenarios. The research highlights the importance of precise feature selection, employing techniques like Principal Component Analysis (PCA), Linear Discriminant Analysis (LDA), and Recursive Feature Elimination (RFE). This research significantly advances the reliability of autonomous driving systems and provides essential insights into fault detection in gear steering systems.

Section: RESEARCH PAPER

Keywords: Fault detection; steering systems; angular acceleration; simulation; wavelet analysis

Citation: Y. Alaraji, S. Alp, An investigation into vibration analysis for detecting faults in vehicle steering outer tie-rod, Acta IMEKO, vol. 13 (2024) no. 1, pp. 1-9. DOI: [10.21014/acta_imeko.v13i1.1742](https://doi.org/10.21014/acta_imeko.v13i1.1742)

Section Editor: Francesco Lamonaca, University of Calabria, Italy

Received January 8, 2024; **In final form** February 21, 2024; **Published** March 2024

Copyright: This is an open-access article distributed under the terms of the Creative Commons Attribution 3.0 License, which permits unrestricted use, distribution, and reproduction in any medium, provided the original author and source are credited.

Corresponding author: Yousif Alaraji, e-mail: yoal-araji@stu.okan.edu.tr

1. INTRODUCTION

The application of Discrete Wavelet Transform (DWT) and Wavelet Scattering in the analysis of vibrational signals in dynamic systems has made significant advancements, replacing conventional methods such as the Fast Fourier Transform (FFT) [1] [2]. These techniques have proven to be robust and effective in fault detection and system analysis, especially when combined with classifiers like Long Short-Term Memory (LSTM) and Support Vector Machines (SVM) [3], [4].

Previous studies have extensively explored methodologies for fault detection in vehicle suspension systems. One such approach utilizes accelerometer sensors on the car body and bogies, demonstrating the effectiveness of PCA-based and CVA-based methods in detecting vertical damper and spring faults [5]. Another study conducted a feasibility analysis of vibration-based fault diagnosis, introducing an FDI unit trained with a functional model-based method. This unit showcased high sensitivity, accurate fault estimation, and robustness to noise and uncertainties in diagnosing faults within railway vehicle suspensions, potentially enhancing safety and performance [6]. A

novel fault diagnosis method leveraging accelerometer data from multiple suspension points was also introduced, demonstrating efficiency through comprehensive simulations using a complete vehicle benchmark. This method offered an effective fault detection solution solely based on accelerometer data [7]. Analysing automobile suspension fatigue employed DWT and wavelet energy analysis, providing valuable insights into evaluating suspension fatigue under varied road conditions and advocating the development of real-time monitoring systems to enhance suspension reliability [8]. Another technique introduced cost-effective fault detection for railway vehicle dampers by analysing phase differences in motion during routine train operations [9]. A proposal has been made to use continuous wavelet transform and Morlet wavelet functions in ADAMS/CAR simulations for detecting damper and upper damper bushing faults in vehicle suspensions. This approach involves observing the changes in natural frequencies and corresponding energy amplitudes, which can enhance fault detection accuracy and improve vehicle suspension fault detection capabilities [10].

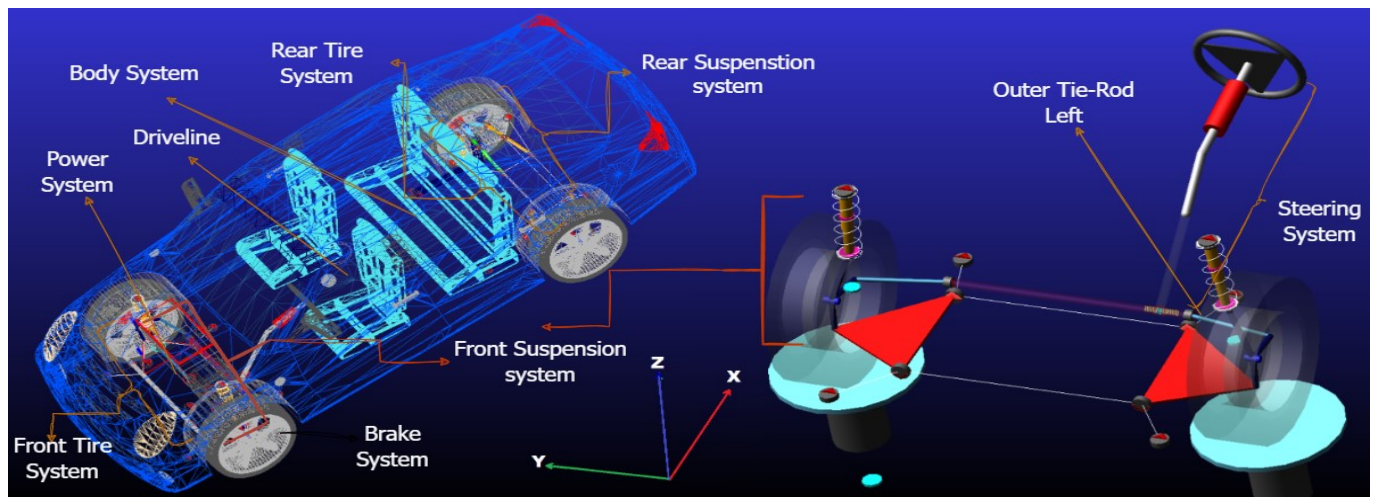


Figure 1. Detailed Examination of Sedan Car's Outer Left Tie Rod via MSC Adams Simulation.

Our research focuses on improving fault detection methodologies for road obstacles and suspension systems through the utilization of advanced machine learning models, specifically Long Short-Term Memory (LSTM) networks, Neural Networks (NN), and Support Vector Machines (SVM). Our focus lies in showcasing the efficacy of SVM and wavelet scattering techniques in capturing nuanced dependencies inherent in sequential data. Additionally, we underscore the robust mathematical underpinnings of these models.

Our investigation involves a comparative analysis between LSTM networks and SVM models, considering factors such as complexity, feature engineering, scalability, interpretability, performance, fault detection accuracy, and processing time. These analyses are performed on a robust hardware setup consisting of an Intel(R) Core (TM) i7-7820HK CPU and an NVIDIA GeForce GTX 1080 GPU to ensure comprehensive evaluations.

To comprehensively analyse the data, we employ techniques such as discrete wavelet transform and wavelet scattering using MATLAB, enabling a holistic approach to explore fault detection across diverse road obstacles.

The study consists of two distinct tests: Road Obstacle Classification across five levels in a noise-free environment; Road Type and Signal Condition Classification in-volving scenarios with noise and subsequent denoising processes; Filtering and method selection to identify the top-performing methods in noisy conditions; and Evaluation of denoising methods to refine result precision while considering fault detection accuracy and processing time.

Additionally, we aim to extract features from signals generated by MSC Adams, simulating varying degrees of loose joints in tie rods and incorporating noise using discrete wavelet transform and wavelet scattering. Subsequently, classifiers such as SVM and LSTM, optimized through various tuners, optimizers, and feature selectors, will be employed to classify these signals based on the degree of loosening, considering fault detection accuracy and processing time.

The analysis of results will determine the most suitable method for our signals, significantly contributing to the advancement of fault detection techniques in suspension systems. Following these experiments, we will meticulously prepare the dataset for feature extraction and thoroughly evaluate fifteen fault detection models.

2. MATERIALS AND METHODS

2.1. Simulation Setup

The study utilized MSC Adams and MATLAB to simulate a front-wheel-drive sedan with ten interconnected systems. The primary focus was on the front Macpherson suspension system, mainly the left outer tie rod (Figure 1).

Signals from this component were analysed extensively.

The car model was integrated into MSC Adams for simulations on a straight road for 20 seconds at 20 km/hr. two specific tests were conducted, examining the angular acceleration of the left outer tie rod along the X-axis under different scenarios:

1. Roughness Obstacle Scenario (Figure 2) - Depicting an 85-meter Uneven Road Sur-face and the Corresponding Output Angular Acceleration Signal.
2. Sine Road Scenario Replication - Displaying an 80-meter Sine Wave-like Obstacle and Corresponding Output Signal.
3. Pothole Obstacle Scenario: Emulated a 10-meter pothole on the road.
4. Bump Obstacle Scenario - Demonstrating a 2-meter Bump with a 7 cm Maximum Height and the Corresponding Output Angular Acceleration Signal.

Angular acceleration data were meticulously collected and processed for each scenario. (Figure 2) depicts the rough road and the collected signal, and the same approach was applied to the other scenarios, resembling real-life accelerometer readings, resulting in four distinct signals.

After the simulation, which lasted for 20 seconds and resulted in the extraction of 1000 instances from each signal, the data in .tab format was transferred to MATLAB for in-depth analysis. This process encompassed signal preprocessing, data labelling, feature extraction, and signal classification. Utilizing MATLAB's robust modelling tools, the analysis was enhanced, facilitating effective interpretation and visualization of the results. This comprehensive analytical approach was crucial in elucidating the effects of various road obstacles on the angular acceleration of the left outer tie rod in the front Macpherson suspension system.

2.2. Data Preparation Operational Modes

2.2.1. First Mode

In this mode, 400 signals are generated, exhibiting a fluctuation range of 0 to 0.002 for normal signals. Deliberate

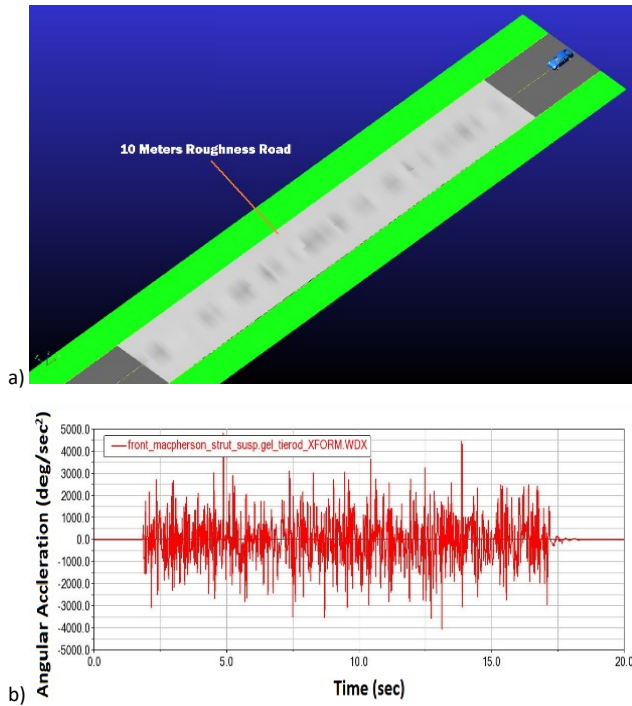


Figure 2. a) Roughness Road Obstacle Scenario, b) Roughness Road: Left Tie-Rod Angular Acceleration Signal.

faults ranging from 0.005 to 2 degrees are introduced across various road type, creating four distinct fault levels, each comprised of 100 signals. These signals undergo meticulous categorization, labelling, and shuffling and are then divided into 80 % for training and 20 % for testing. Following categorization, the data is processed for feature extraction. Fifteen fault detection models under-go evaluation, with the most accurate ones subjected to a two-step testing process involving the introduction of noise to simulate grainy road conditions and

subsequent denoising testing to gauge their resilience and effectiveness.

2.2.2. Second Mode

This mode represents healthy and worn conditions and employs 400 healthy signals per road type. It simulates wear ranging from no wear to 0.001 and faults spanning from 0.005 to 2 degrees. These signals are appropriately labelled, shuffled, and divided into training and testing sets. The dataset is then readied for feature extraction. Fifteen fault detection models undergo evaluation across two scenarios: Signals affected by added noise mimicking a grainy road surface, and signals pre-processed through denoising before testing, providing a comprehensive assessment of their performance under different conditions.

2.3. Features Extraction

2.3.1. Discrete wavelet transformation DWT

The Discrete Wavelet Transform (DWT) is a versatile mathematical technique employed in image processing, signal compression, and feature extraction [11]. Unlike the Fourier Transform, DWT dissects data into different scales using wavelets [12], specifically using the Daubechies 4 (db4) wavelet in this instance with a decomposition level of 5 (Figure 3), exemplifying its application on the rough road signal.

The DWT utilizes a filter bank with low-pass (LPF) and high-pass filters (HPF) to selectively capture low-frequency and high-frequency components of the signal [13], followed by down sampling.

The core equation for DWT involves the wavelet function:

$$DWT_{\varphi}(j, k) = \int_{-\infty}^{\infty} s(t) \varphi_{j,k}^{*}(t) dt. \quad (1)$$

The Discrete Wavelet Transform $DWT_{\varphi}(j, k)$ assesses the correlation between a signal $s(t)$ and a transformed wavelet function $\varphi_{j,k}^{*}(t)$ that is both scaled and shifted across time. This computation reveals the signal's energy or information content at specific scales (j) and time positions (k) in signal analysis. The function $\varphi_{j,k}^{*}(t)$ is derived from basic wavelets ϕ and $\psi(0)$, providing a versatile tool to analyse signals across various scales and time points in signal processing.

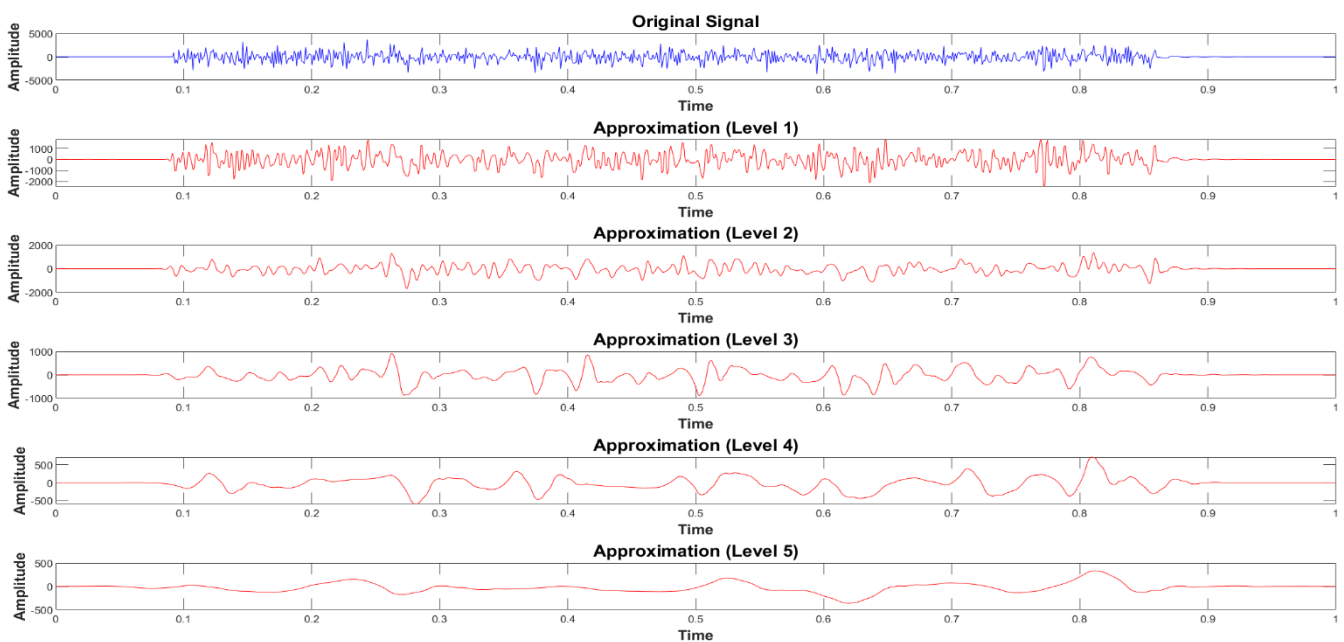


Figure 3. Discrete Wavelet Five Levels (Wavelet Db4).

The hierarchical structure of the DWT allows for Multi-resolution Analysis (MRA) at multiple scales, representing different resolutions of the signal [14]. In a 5-level DWT with the 'db4' wavelet applied to a signal of length 1000, the estimated number of coefficients extracted from each level are as follows [12]: Level 1 has 503 coefficients, Level 2 has 251 coefficients, Level 3 comprises 125 coefficients, Level 4 includes 62 coefficients, and Level 5 consists of 31 coefficients (Figure 3). The total number of features (wavelet coefficients) extracted from each signal after the 5-level DWT is approximately 1003, encompassing both detail and approximation coefficients from all levels.

2.4. Wavelet Scattering

Wavelet scattering, akin to a deep convolutional network, extracts low-variance features from time series and images, emphasizing translation invariance and resilience to time warping [15]. Effective in classification, it dissects signals into scales and orientations, excelling in diverse signal analyses and texture classification, including electromagnetic signals [16]-[17]. The method decomposes signals into scales and orientations via wavelet operations, providing stable, translation-invariant representations. In a specific application, 20 invariant features yield 588 features per signal, enabling detailed analysis. In Continuous Wavelet Transform (CWT), first-order scattering coefficients involve 'temporal averaging,' crucial for stability [18],[19]. (Refer to Figure 4), demonstrating its usage on the signal from the rough road.

The wavelet scattering transform, denoted as S_m , involves a strategic process to ensure stability against time-warping deformations and introduces time-shift variance:

$$S_mx(t, \lambda_1, \lambda_2, \dots, \lambda_m) = |x * \varphi_{\lambda_1}| * \dots * \varphi_{\lambda_m} * \phi. \quad (2)$$

Here, x is the input signal, φ_{λ_i} represents wavelet functions at different scales λ_i , and ϕ denotes the low-pass filter used for averaging after the convolution with the m-th order wavelets.

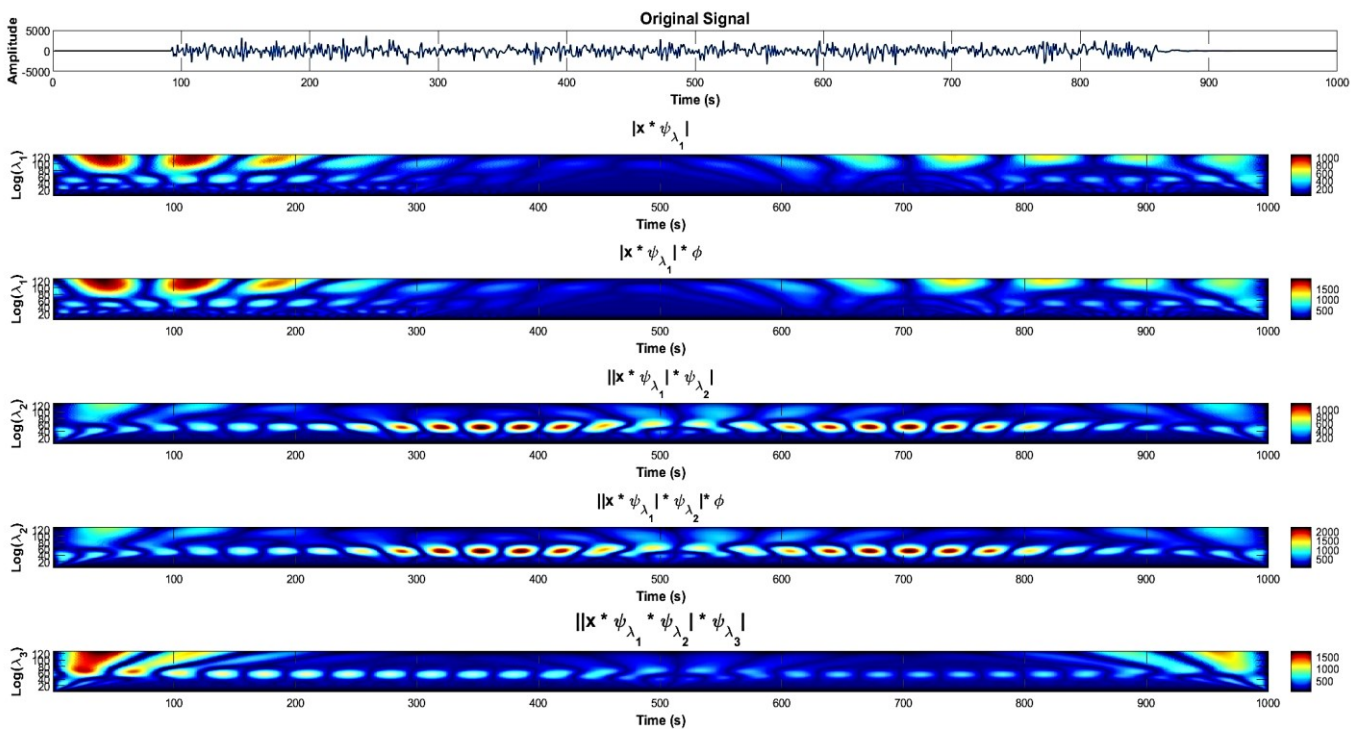


Figure 4. Wavelet Scattering Time-Frequency Convolution Process

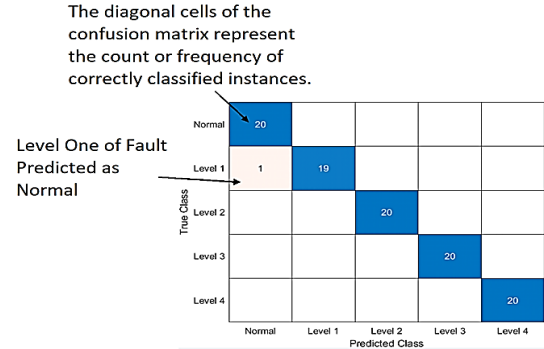


Figure 5. Four Faulty Levels Classification

The process captures information across multiple scales and orientations, preserving energy between time and frequency domains [18].

2.5. Classifiers

Support Vector Machines (SVM) and Neural Networks (NN) are employed in this research to develop a fault detection and classification system for a vehicle's tie rod - a critical steering component. The goal is accurate detection and classification of tie rod faults, crucial for ensuring vehicle safety and performance.

1. Classifying Four Fault Levels: SVM and NN are used to categorize tie rod faults into four levels, aiding in targeted maintenance actions based on fault severity. Detailed classification provides a comprehensive understanding of the tie rod's condition (Figure 5).
2. Detecting 'Faulty' or 'Normal' Conditions: SVM and NN are employed to discern tie rod conditions as 'faulty' or 'normal' when encountering various road obstacles like sinewave, grid, pothole, and bump obstacles. This analysis helps identify abnormalities based on tie rod responses (Figure 6).

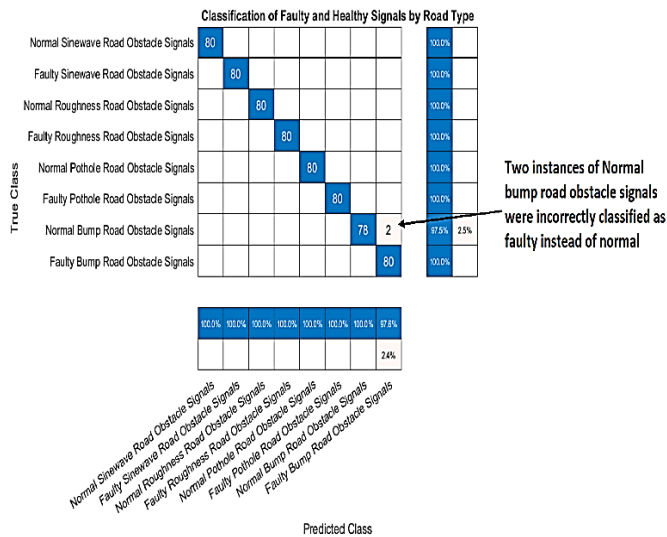


Figure 6. Four Faulty Levels Classification

2.5.1. Support Vector Machines (SVM)

Support Vector Machines (SVM) are a powerful tool for classification and regression tasks, with the ability to handle nonlinear data through kernelization [20]. The SVM kernelization equation is commonly represented as:

$$f(x) = w^T k(x, x') + b = 0. \quad (3)$$

Here, w is the weight vector, which is a linear combination of the support vector. The kernel function is denoted by $k(x, x')$, and it implicitly defines the mapping to the higher-dimensional space, capturing the essence of kernelization. and the bias term b contributes to the decision boundary in this transformed space. In the context of SVM, kernelization plays a crucial role in transforming data into a higher-dimensional space using functions like polynomial, Gaussian, or sigmoid kernels. This technique is particularly useful for addressing nonlinear patterns in data [20].

The research implemented Support Vector Machines (SVM) using MATLAB, incorporating specific hyperparameters such as Box Constraint and Kernel Scale for optimization. A systematic exploration of these parameters was conducted, as depicted in (Figure 7), to enhance overall performance. It's crucial to emphasize that the adjustment of these hyperparameters aims to fine-tune the SVM model, leading to improved accuracy and generalization. This methodological approach is applied specifically to enhance the road fault detection and classification within the scope of the research.

2.5.2. Long Short-Term Memory (LSTM)

Long Short-Term Memory (LSTM) networks are a specialized type of Recurrent Neural Networks (RNNs) designed for processing sequential data while addressing the challenge of capturing long-term dependencies [21].

In this project, LSTM networks were employed to proficiently model sequential data through MATLAB. The LSTM configuration included 1500 hidden units, adept at capturing intricate temporal patterns. The training process spanned 170 epochs, employing a batch size of 170 to strike a balance between learning efficiency and computational resources. To mitigate overfitting, a validation strategy was implemented, evaluating the model every 30 epochs.

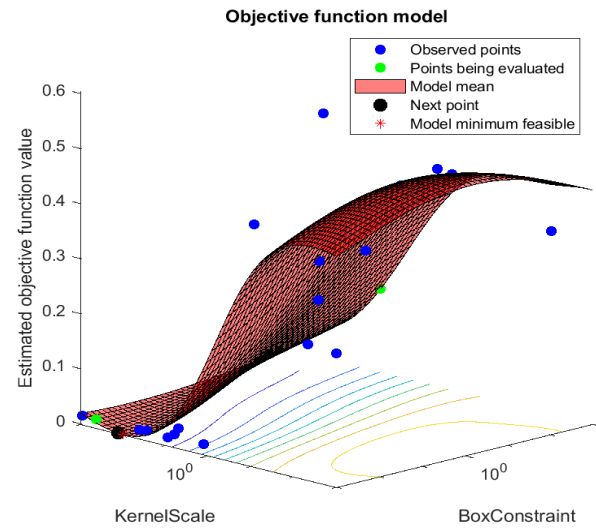


Figure 7. Objective Function Modelling of a faulty and healthy signal for each road type.

The LSTM architecture was specified using a sequence input layer and an LSTM layer with 1500 hidden units, complemented by additional layers for classification. The 'adam' optimizer was chosen for its effectiveness during training.

The training was orchestrated via the `trainNetwork` function, incorporating the training features (`TrainFeatures`) and corresponding labels (`YTrain`). Post-training, predictions on the test set were generated using the `classify` function.

These MATLAB implementations effectively optimized the LSTM network for the complexity of the sequential data, showcasing its prowess in accurately modelling and predicting intricate sequences in the project.

3. RESULTS

3.1. Test 1: Road Obstacle Fault Detection in Noisy Environments

In our initial road obstacle fault detection test, we rigorously examined 15 diverse methods in a noisy environment, classifying each obstacle into five fault levels, including the normal condition. The primary goal was to identify fault levels for Sinewave, Grid, Pothole, and Bump obstacles. Findings from the noisy environment, summarized in Table 1, provided valuable insights. Notably, the Wavelet Scattering SVM PCA method exhibited exceptional performance with a mean accuracy of 99.1 %, emphasizing its robustness in detecting fault levels in noisy conditions. The assessment shed light on the trade-offs between detection accuracy and operational efficiency. Some methods, such as Wavelet Scattering SVM Tuned DWT with SVM, also demonstrated strong performance in the test, albeit with a slight increase in processing time. This underscores the importance of striking a balance between accuracy and efficiency in road safety applications, especially when discerning fault levels for different obstacles.

3.2. Test 2: Road Obstacle Fault Detection in Denoised Environments

Continuing our investigation, we focused on assessing road obstacle detection under denoised conditions, with the goal of identifying the fault level for each obstacle. Using the same set of 15 methods and leveraging MATLAB's "wdenoise" function, we aimed to understand how denoising impacted the accuracy and efficiency of each method across different obstacles and fault levels, including the normal condition. Table 2 presents the

results of the evaluation in the denoised environment. The Wavelet Scattering SVM PCA method continued to shine, maintaining top-tier accuracy post-denoising in accurately identifying the fault level for various obstacles, including the normal condition. This finding underscores the model's robustness, demonstrating its capability to deliver consistent performance even after denoising. However, it's important to note that certain methods, such as Wavelet Scattering SVM Tuned RFE and Tuned, exhibited improvement after denoising at the expense of increased processing time. This observation emphasizes the delicate balance required in road safety applications, where accurately identifying the fault level for different obstacles remains a critical objective.

3.3. Test 3: Road Obstacles and Health Condition Classification in Noisy Environments

The third test aimed to comprehensively classify road obstacles and signal conditions (healthy or faulty) under noisy conditions. The overarching objective was to maximize accuracy while minimizing processing time. The evaluation encompassed diverse noisy scenarios, employing 15 different methods to classify all previously identified obstacles. The results, as outlined

in Table 3, showcased the Wavelet Scattering RNN ADAM model, which maintained a high mean accuracy of 97.8% with a relatively low standard deviation. The Wavelet Scattering RNN ADAM model displayed outstanding performance and consistency in noisy conditions, essential for effective road safety applications. Test 3 outcomes emphasized the importance of accurate classification for road types and signal conditions in noisy environments. The model reliably navigated obstacles and signals in noisy conditions, showcasing robust performance.

3.4. Test 4: Road Obstacles and Health Condition Classification in Denoised Environments

The fourth test was dedicated to the classification of road obstacles and signal conditions (healthy or faulty) in denoised conditions. Mirroring the objectives of Test 3, the goal was to maximize accuracy while minimizing processing time. The evaluation spanned various denoised scenarios, employing the same 15 methods across all obstacles. The results, presented in Table 4, identified the Wavelet Scattering SVM Tuned LDA model as a top performer with a mean accuracy of 98.4%. Increased processing time impacted road safety systems, highlighting the accuracy-time trade-off. Test 4 emphasized

Table 1. First Test Method Performance Summary (With Noises).

| Model Name | Number of Training Cycles | Mean Accuracy (%) | Std Accuracy (%) | CI Lower Accuracy (%) | CI Upper Accuracy (%) | Mean Time (s) | Std Time (s) | CI Lower Time (s) | CI Upper Time (s) |
|----------------------------------|---------------------------|-------------------|------------------|-----------------------|-----------------------|---------------|--------------|-------------------|-------------------|
| Wavelet Scattering SVM PCA | 5 Folds | 99.1 | 0.144 | 98.9 | 99.4 | 11 | 1 | 9 | 13 |
| DWT SVM | 1 Iteration | 95.0 | 2.16 | 91.6 | 98.4 | 9 | 4 | 3 | 15 |
| Wavelet Scattering SVM Tuned | 20 Evaluations | 95.0 | 1.41 | 92.7 | 97.3 | 403 | 62 | 304 | 503 |
| Wavelet Scattering SVM CV SRE | 5 Folds | 94.9 | 2.66 | 90.6 | 99.1 | 11 | 1 | 9 | 13 |
| Wavelet Scattering RNN ADAM | 170 Epochs | 94.8 | 1.50 | 92.4 | 97.1 | 53 | 3 | 49 | 58 |
| Wavelet Scattering SVM Tuned SRE | 20 Evaluations | 94.5 | 1.29 | 92.4 | 96.6 | 183 | 75 | 65 | 302 |
| DWT SVM Tuned | 20 Evaluations | 94.3 | 1.26 | 92.2 | 96.3 | 382 | 346 | 169 | 932 |
| Wavelet Scattering SVM CV | 5 Folds | 94.3 | 1.55 | 91.8 | 96.7 | 22 | 20 | 10 | 54 |
| Wavelet Scattering RNN | 170 Epochs | 93.8 | 2.63 | 89.6 | 97.9 | 59 | 4 | 52 | 66 |
| Wavelet Scattering SVM Tuned RFE | 20 Evaluations | 93.0 | 1.41 | 90.7 | 95.3 | 123 | 14 | 100 | 145 |
| Wavelet Scattering SVM CV RFE | 5 Folds | 91.1 | 0.625 | 90.1 | 92.1 | 13 | 1 | 12 | 15 |
| DWT SVM SRE Tuned | 20 Evaluations | 91.0 | 2.94 | 86.3 | 95.7 | 487 | 403 | 154 | 1130 |
| Wavelet Scattering SVM CV LDA | 5 Folds | 77.0 | 5.72 | 67.9 | 86.1 | 9 | 1 | 8 | 10 |
| Wavelet Scattering SVM Tuned LDA | 20 Evaluations | 68.0 | 7.16 | 56.6 | 79.4 | 83 | 2 | 79 | 87 |
| DWT Neural Network | 200 Epochs | 54.0 | 6.00 | 44.5 | 63.5 | 10 | 9 | 5 | 24 |

Table 2. Second Test Method Performance Summary (Denoised).

| Model Name | Number of Training Cycles | Mean Accuracy (%) | Std Accuracy (%) | CI Lower Accuracy (%) | CI Upper Accuracy (%) | Mean Time (s) | Std Time (s) | CI Lower Time (s) | CI Upper Time (s) |
|----------------------------------|---------------------------|-------------------|------------------|-----------------------|-----------------------|---------------|--------------|-------------------|-------------------|
| Wavelet Scattering SVM PCA | 5 Folds | 97.9 | 2.750 | 93.5 | 100.0 | 11 | 7 | 1 | 22 |
| Wavelet Scattering SVM Tuned RFE | 20 Evaluations | 97.6 | 1.110 | 95.9 | 99.4 | 91 | 16 | 65 | 116 |
| Wavelet Scattering SVM Tuned | 20 Evaluations | 97.3 | 0.655 | 96.2 | 98.3 | 565 | 368 | 20 | 1150 |
| Wavelet Scattering SVM Tuned SRE | 20 Evaluations | 96.0 | 0.816 | 94.7 | 97.3 | 146 | 25 | 107 | 185 |
| Wavelet Scattering RNN ADAM | 170 Epochs | 96.0 | 2.000 | 92.8 | 99.2 | 53 | 1 | 51 | 55 |
| Wavelet Scattering SVM CV RFE | 5 Folds | 94.8 | 0.315 | 94.3 | 95.3 | 13 | 1 | 11 | 14 |
| Wavelet Scattering RNN | 170 Epochs | 94.5 | 0.577 | 93.6 | 95.4 | 54 | 1 | 52 | 56 |
| DWT SVM | 1 Iteration | 94.5 | 1.290 | 92.4 | 96.6 | 5 | 2 | 2 | 9 |
| DWT SVM Tuned | 20 Evaluations | 93.5 | 3.700 | 87.6 | 99.4 | 361 | 189 | 61 | 661 |
| Wavelet Scattering SVM CV SRE | 5 Folds | 93.4 | 0.903 | 92.0 | 94.9 | 12 | 5 | 3 | 20 |
| Wavelet Scattering SVM CV | 5 Folds | 93.3 | 0.772 | 92.1 | 94.5 | 18 | 8 | 5 | 31 |
| DWT SVM SRE Tuned | 20 Evaluations | 90.5 | 2.080 | 87.2 | 93.8 | 561 | 444 | 145 | 1270 |
| Wavelet Scattering SVM CV LDA | 5 Folds | 84.9 | 10.200 | 68.7 | 100.0 | 8,5 | 0,5 | 8 | 9 |
| DWT Neural Network | 200 Epochs | 82.0 | 3.460 | 76.5 | 87.5 | 247 | 41 | 182 | 311 |
| Wavelet Scattering SVM Tuned LDA | 20 Evaluations | 73.3 | 10.600 | 56.4 | 90.1 | 84 | 2 | 81 | 86 |

precise classification in denoised conditions, with the Wavelet Scattering SVM Tuned LDA model showcasing high accuracy, emphasizing the balance between precision and efficiency in real-world applications.

4. DISCUSSION

This study's evaluation of road obstacle detection methods encompassed various signal conditions, noise scenarios, and denoising techniques, targeting enhancements in autonomous driving and road safety. A key finding was the exceptional performance of "Wavelet Scattering SVM PCA" in fault levels detection, paralleling its effectiveness in vibration fault diagnosis for bearings at variable speeds [22]. Additionally, the combination of wavelet scattering with LSTM proved effective in classifying unbalanced and bowed rotors [23], while "Wavelet SVM Tuned (LDA)" showed promise in mixed signal environments, akin to its application in bearing vibration fault detection [24].

In noisy conditions, "Wavelet Scattering SVM Tuned" demonstrated robustness, particularly in detecting unbalanced and bowed rotors [23], underscoring the significance of careful

feature selection. Across all tests, "Wavelet Scattering LSTM Tuned" emerged as the most stable method in our research, highlighting the importance of tailored feature selection and adaptive techniques for effective road obstacle detection in autonomous driving systems.

Future research should focus on integrating LiDAR with accelerometers, combined with wavelet scattering and classification techniques. Inspired by the use of LiDAR in earthquake detection [25] and the incorporation of finite element analysis with vibration fault detection in defected ball bearings [26], this approach could yield more precise detection results. Investment in advanced hardware and comparative studies of machine-learning algorithms are also recommended.

Implementing these recommendations enhances fault detection accuracy and practicality, benefiting the automotive industry in manufacturing, fleet management, road safety, and aftermarket services. This contributes to improved safety, reduced maintenance costs, and heightened operational efficiency.

Table 3. Third Test: Summary of Method Performance Metric (With Noise).

| Model Name | Number of Training Cycles | Mean Accuracy (%) | Std Accuracy (%) | CI Lower Accuracy (%) | CI Upper Accuracy (%) | Mean Time (s) | Std Time (s) | CI Lower Time (s) | CI Upper Time (s) |
|----------------------------------|---------------------------|-------------------|------------------|-----------------------|-----------------------|---------------|--------------|-------------------|-------------------|
| Wavelet Scattering RNN ADAM | 170 Epochs | 97.8 | 0.776 | 95.9 | 99.7 | 360 | 79 | 164 | 556 |
| DWT Neural Network | 200 Epochs | 97.7 | 0.261 | 97.0 | 98.3 | 41 | 6 | 25 | 57 |
| Wavelet Scattering SVM Tuned SRE | 20 Evaluations | 97.5 | 0.304 | 96.7 | 98.3 | 2970 | 530 | 1660 | 4290 |
| Wavelet Scattering SVM CV | 5 Folds | 97.2 | 0.846 | 95.1 | 99.3 | 86 | 17 | 44 | 128 |
| Wavelet Scattering SVM CV SRE | 5 Folds | 97.1 | 0.463 | 95.9 | 98.2 | 91 | 12 | 62 | 119 |
| Wavelet Scattering SVM CV RFE | 5 Folds | 96.5 | 0.087 | 96.2 | 96.7 | 73 | 13 | 42 | 104 |
| Wavelet Scattering SVM Tuned RFE | 20 Evaluations | 96.3 | 0.135 | 95.9 | 96.6 | 2010 | 406 | 999 | 3010 |
| Wavelet Scattering SVM PCA | 5 Folds | 95.8 | 0.610 | 94.3 | 97.3 | 81 | 14 | 46 | 116 |
| Wavelet Scattering SVM Tuned LDA | 20 Evaluations | 95.6 | 0.367 | 94.7 | 96.5 | 224 | 42 | 121 | 328 |
| Wavelet Scattering RNN | 170 Epochs | 95.5 | 0.685 | 93.7 | 97.2 | 386 | 56 | 248 | 524 |
| Wavelet Scattering SVM CV LDA | 5 Folds | 95.4 | 0.200 | 94.9 | 95.9 | 62 | 12 | 32 | 92 |
| Wavelet Scattering SVM Tuned | 20 Evaluations | 95.3 | 0.735 | 93.5 | 97.1 | 2630 | 483 | 1430 | 3830 |
| DWT SVM Tuned | 20 Evaluations | 95.0 | 0.598 | 93.5 | 96.5 | 4590 | 486 | 3380 | 5800 |
| DWT SVM SRE Tuned | 20 Evaluations | 93.1 | 0.304 | 92.4 | 93.9 | 4420 | 836 | 2340 | 6500 |
| DWT SVM | 1 Iteration | 92.2 | 0.358 | 91.3 | 93.1 | 194 | 38 | 99 | 290 |

Table 4. Fourth Test: Summary of Method Performance Metric (Denoised).

| Model Name | Number of Training Cycles | Mean Accuracy (%) | Std Accuracy (%) | CI Lower Accuracy (%) | CI Upper Accuracy (%) | Mean Time (s) | Std Time (s) | CI Lower Time (s) | CI Upper Time (s) |
|----------------------------------|---------------------------|-------------------|------------------|-----------------------|-----------------------|---------------|--------------|-------------------|-------------------|
| Wavelet Scattering SVM Tuned LDA | 20 Evaluations | 98.4 | 0.348 | 97.6 | 99.3 | 219 | 46 | 104 | 334 |
| Wavelet Scattering SVM Tuned | 20 Evaluations | 98.4 | 0.481 | 97.2 | 99.6 | 3580 | 602 | 2080 | 5080 |
| Wavelet Scattering SVM Tuned SRE | 20 Evaluations | 98.3 | 0.180 | 97.8 | 98.7 | 3400 | 691 | 1680 | 5110 |
| Wavelet Scattering SVM Tuned RFE | 20 Evaluations | 98.3 | 0.289 | 97.6 | 99.0 | 3760 | 569 | 2340 | 5170 |
| Wavelet Scattering RNN ADAM | 170 Epochs | 98.3 | 0.382 | 97.3 | 99.2 | 363 | 18 | 317 | 408 |
| DWT Neural Network | 200 Epochs | 98.1 | 0.499 | 96.9 | 99.4 | 44 | 3 | 36 | 52 |
| Wavelet Scattering SVM CV SRE | 5 Folds | 97.8 | 0.450 | 96.7 | 98.9 | 123 | 19 | 77 | 169 |
| Wavelet Scattering SVM CV LDA | 5 Folds | 97.7 | 0.456 | 96.6 | 98.9 | 60 | 12 | 29 | 91 |
| Wavelet Scattering RNN | 170 Epochs | 97.7 | 0.576 | 96.2 | 99.1 | 355 | 14 | 321 | 389 |
| Wavelet Scattering SVM CV RFE | 5 Folds | 97.4 | 0.170 | 97.0 | 97.8 | 71 | 11 | 43 | 99 |
| Wavelet Scattering SVM CV | 5 Folds | 97.1 | 0.551 | 95.8 | 98.5 | 114 | 22 | 59 | 168 |
| DWT SVM Tuned | 20 Evaluations | 97.0 | 0.439 | 95.9 | 98.1 | 4420 | 861 | 2280 | 6560 |
| DWT SVM SRE Tuned | 20 Evaluations | 95.9 | 0.421 | 94.9 | 97.0 | 1560 | 269 | 894 | 2230 |
| Wavelet Scattering SVM PCA | 5 Folds | 92.9 | 0.520 | 91.6 | 94.2 | 551 | 101 | 299 | 803 |
| DWT SVM | 1 Iteration | 92.5 | 0.410 | 91.5 | 93.5 | 190 | 28 | 120 | 260 |

5. CONCLUSION

The research work focuses on detecting suspension failure in a simulated car's steering system, a critical factor causing road accidents. It employs simulation, data analysis, signal processing, and classification techniques.

Key findings encompass simulating wear in the outer tie rod, utilizing methods like wavelet scattering and discrete wavelet transform for feature extraction, and employing Support Vector Machines (SVM) and Neural Networks (NN) for signal classification. Across all the tests conducted, "Wavelet Scattering" stood out for feature extraction, while "LSTM" (Long Short-Term Memory) networks demonstrated high efficiency in classification. Moreover, the study notably highlighted the proficiency of "Wavelet Scattering LSTM Tuned" in ensuring accurate classification in diverse scenarios.

The study emphasizes the necessity for diverse datasets and real-world testing to enhance fault detection accuracy while acknowledging limitations in the simulated environment.

This research is pivotal for enhancing automotive safety by providing methodologies relevant to real-world scenarios, paving the way for advancements in steering system fault detection and overall road safety.

In summary, the research emphasizes tailored approaches based on data characteristics and noise levels for effective road obstacle detection. It aims to reduce suspension-related accidents and advance autonomous driving technology for safer roads.

REFERENCES

- [1] A. A. Al Tace, R. N. Khushaba, T. Zia, A. Al-Jumaily, The Effectiveness of Narrowing the Window size for LD & HD EMG Channels based on Novel Deep Learning Wavelet Scattering Transform Feature Extraction Approach, 44th Annual International Conference of the IEEE, 2022, pp. 3698–3701. DOI: [10.1109/EMBEC48229.2022.9871473](https://doi.org/10.1109/EMBEC48229.2022.9871473)
- [2] D. L. Rani, M. Bharathi, N. Padmaja, Performance Comparison of FFT, DCT, DWT and DDDWT-OFDM in Rayleigh Channel, 2019 International Conference on Smart Systems and Inventive Technology (ICSSIT), 2019, pp. 392–394. DOI: [10.1109/ICSSIT46314.2019.8987953](https://doi.org/10.1109/ICSSIT46314.2019.8987953)
- [3] F. Liu, Sh. Xia, Sh. Wei, L. Chen, Y. Ren, X. Ren, Zh. Xu, S. Ai, Ch. Liu, Wearable electrocardiogram quality assessment using wavelet scattering and LSTM, Front Physiol, vol. 13, 2022, p. 905447. DOI: [10.3389/fphys.2022.905447](https://doi.org/10.3389/fphys.2022.905447)
- [4] E. S. Fonseca, R. C. Guido, A. C. Silvestre, J. C. Pereira, Discrete wavelet transform and support vector machine applied to pathological voice signals identification, 7th IEEE International Symposium on Multimedia (ISM05), 2005, pp. 5. DOI: [10.1109/ISM.2005.50](https://doi.org/10.1109/ISM.2005.50)
- [5] X. Wei, L. Jia, H. Liu, A comparative study on fault detection methods of rail vehicle suspension systems based on acceleration measurements, Vehicle System Dynamics, vol. 51, no. 5, 2013, pp. 700–720. DOI: [10.1080/00423114.2013.767464](https://doi.org/10.1080/00423114.2013.767464)
- [6] J. S. Sakellariou, K. A. Petsounis, S. D. Fassois, Vibration based fault diagnosis for railway vehicle suspensions via a functional model-based method: A feasibility study, Journal of Mechanical Science and Technology, vol. 29, no. 2, Nov. 2015, pp. 471–484. DOI: [10.1007/s12206-015-0107-0](https://doi.org/10.1007/s12206-015-0107-0)
- [7] S. Yin, Z. Huang, Performance Monitoring for Vehicle Suspension System via Fuzzy Positivistic C-Means Clustering Based on Accelerometer Measurements, IEEE/ASME Transactions on Mechatronics, vol. 20, no. 5, Nov. 2015, pp. 2613–2620. DOI: [10.1109/TMECH.2014.2358674](https://doi.org/10.1109/TMECH.2014.2358674)
- [8] A. A. A. Rahim, S. Abdullah, S. S. K. Singh, M. Z. Nuawi, Selection of the optimum decomposition level using the discrete wavelet transform for automobile suspension system, Journal of Mech. Science and Technology, vol. 34, no. 1, Nov. 2020, pp. 137–142. DOI: [10.1007/s12206-019-1213-1](https://doi.org/10.1007/s12206-019-1213-1)
- [9] T. Kojima, Y. Sugahara, Fault Detection of Vertical Dampers of Railway Vehicle Based on Phase Difference of Vibrations, vol. 54, no. 3, 2013, pp. 139–144. DOI: [10.2219/rtrigr.54.139](https://doi.org/10.2219/rtrigr.54.139)
- [10] S. Azadi, A. Soltani, Fault detection of vehicle suspension system using wavelet analysis, Vehicle System Dynamics, vol. 47, no. 4, Nov. 2009, pp. 403–418. DOI: [10.1080/00423110802094298](https://doi.org/10.1080/00423110802094298)
- [11] S. G. Mallat, G. Peyré, A wavelet tour of signal processing: the sparse way. 1999. DOI: [10.1016/B978-0-12-374370-1.X0001-8](https://doi.org/10.1016/B978-0-12-374370-1.X0001-8)
- [12] S. G. Mallat, A Theory for Multiresolution Signal Decomposition: The Wavelet Representation, IEEE Trans Pattern Anal Mach Intell, vol. 1, no. 7, 1989, DOI: [10.1109/34.192463](https://doi.org/10.1109/34.192463)
- [13] Geoffrey C. Green, Wavelet-based denoising of cardiac PET data. Library and Archives Canada, Bibliothèque et Archives Canada, 2005. DOI: [10.22215/etd/2005-07963](https://doi.org/10.22215/etd/2005-07963)
- [14] V. S. Chourasia, A. K. Tiwari, Design methodology of a new wavelet basis function for fetal phonocardiographic signals, The Scientific World Journal, vol. 2013, 2013, Article ID 505840. DOI: [10.1155/2013/505840](https://doi.org/10.1155/2013/505840)
- [15] S. Mallat, Group Invariant Scattering, Commun Pure Appl Math, vol. 65, no. 10, Nov. 2012, pp. 1331–1398. DOI: [10.1002/cpa.21413](https://doi.org/10.1002/cpa.21413)
- [16] C. Szegedy, W. Liu, Y. Jia, P. Sermanet, S. Reed, D. Anguelov, D. Erhan, V. Vanhoucke, A. Rabinovich, IEEE Conf. on Computer Vision and Pattern Recognition (CVPR), IEEE Computer Society, 2015, pp. 1–9. DOI: [10.1109/CVPR.2015.7298594](https://doi.org/10.1109/CVPR.2015.7298594)
- [17] J. Bruna, S. Mallat, Invariant scattering convolution networks, IEEE Trans Pattern Anal Mach Intell, vol. 35, no. 8, 2013, pp. 1872–1886. DOI: [10.1109/TPAMI.2012.230](https://doi.org/10.1109/TPAMI.2012.230)
- [18] J. Andén, S. Mallat, Deep scattering spectrum, IEEE Transactions on Signal Processing, vol. 62, no. 16, Nov. 2014, pp. 4114–4128. DOI: [10.1109/TSP.2014.2326991](https://doi.org/10.1109/TSP.2014.2326991)
- [19] Y. Zhang, L. Wu, Classification of fruits using computer vision and a multiclass support vector machine, Sensors (Switzerland), vol. 12, no. 9, Nov. 2012, pp. 12489–12505. DOI: [10.3390/s120912489](https://doi.org/10.3390/s120912489)
- [20] Í. Santana, B. Serrano, M. Schiffer, T. Vidal, Support Vector Machines with the Hard-Margin Loss: Optimal Training via Combinatorial Benders' Cuts, Nov. 2022, 23 pp. DOI: [10.48550/arXiv.2207.07690](https://doi.org/10.48550/arXiv.2207.07690)
- [21] H. Sak, A. Senior, F. Beaufays, Long Short-Term Memory Based Recurrent Neural Network Architectures for Large Vocabulary Speech Recognition, Nov. 2014, 5 pp. DOI: [10.48550/arXiv.1402.1128](https://doi.org/10.48550/arXiv.1402.1128)
- [22] M. Pule, O. Matsebe, R. Samikannu, Application of PCA and SVM in Fault Detection and Diagnosis of Bearings with Varying Speed, Math Probl Eng, vol. 2022, p. 5266054. DOI: [10.1155/2022/5266054](https://doi.org/10.1155/2022/5266054)
- [23] N. Rezazadeh, M. de Oliveira, D. Perfetto, A. De Luca, F. Caputo, Classification of Unbalanced and Bowed Rotors under Uncertainty Using Wavelet Time Scattering, LSTM, and SVM. Appl. Sci. 2023, 13, 6861. DOI: [10.3390/app13126861](https://doi.org/10.3390/app13126861)
- [24] Josué Pacheco-Chérrez, Jesús A. Fortoul-Díaz, Cortés-Santacruz, Froylán, Alosa-Valerdi, Luz María, Ibarra-Zarate, I. David, Bearing fault detection with vibration and acoustic signals: Comparison among different machine learning classification methods, Engineering Failure Analysis, vol. 139, 2022, 106515. DOI: [10.1016/j.engfailanal.2022.106515](https://doi.org/10.1016/j.engfailanal.2022.106515)

- [25] A. K. Krishnan, E. Nissen, S. Saripalli, R. Arrowsmith, A. H. Corona, Change Detection Using Airborne LiDAR: Applications to Earthquakes. In: Desai, J., Dudek, G., Khatib, O., Kumar, V. (eds) Experimental Robotics. Springer Tracts in Advanced Robotics, vol 88. Springer, Heidelberg.
DOI: [10.1007/978-3-319-00065-7_49](https://doi.org/10.1007/978-3-319-00065-7_49)
- [26] V. G. Salunkhe, R. G. Desavale, Surajkumar G. Kumbhar, Vibration Analysis of Deep Groove Ball Bearing Using Finite Element Analysis and Dimension Analysis. Journal of Tribology, 144(8), 081202 (18 pages).
DOI: [10.1115/1.4053262](https://doi.org/10.1115/1.4053262)